International Journal of
Mathematics And its Applications
ISSN: 2347-1557

Int. J. Math. And Appl., **11(4)**(2023), 181–196
Available Online: http://ijmaa.in

Forced Convective Heat Transfer in Magnetohydrodynamic Boundary Layer Flow Under Slip Boundary Condition

T. N. Vasanthakumari[1,*]

[1]*Department of Mathematics, Government First Grade College, Tumakuru, Karnataka, India*

Abstract

This paper examines the magnethydrodynamic boundary layer flow and associated forced convective heat transfer over a permeable wedge with the slip velocity and viscous dissipation on an the electrically conducting fluid. It is considered that a magnetic field is applied normally to the flow direction, and the wedge velocity and mainstream flow are both functions of distance along the wedge wall. Applying the appropriate similarity transformations to a set of Prandtl boundary layer equations, the modeled system of ordinary differential equations are obtained. The shooting algorithm which is a combination of Runge-Kutta and secant method is used to solve these governing equations. Numerical results demonstrate that the boundary layer thickness, velocity and temperature profiles are greatly influenced by the pressure gradient, Hartmann number, slip velocity, Prandtl number and Eckert number. In particular, both momentum and thermal boundary layer thicknesses are thin for which velocity and temperature profiles are benign. The interesting physical mechanisms are discussed in detail.

Keywords: Boundary layer flows; Slip velocity; Eckert number; Shooting technique; Hartman number.
2020 Mathematics Subject Classification: 76D10, 80A21.

1. Introduction

The study of electrically conducting fluid flow and heat transfer over a wedge surface under the influence of an applied magnetic field is a complex problem involving the interplay of various physical phenomena. The pressure gradient, slip velocity, and viscous dissipation each play a significant role in determining the behavior of the momentum and thermal boundary layers.

The pressure gradient, arising from the wedge geometry and the variation in mainstream velocity, influences the fluid flow by accelerating or decelerating the fluid particles. This, in turn, affects the thickness of the momentum boundary layer and the distribution of velocity within it. The slip velocity,

*Corresponding author (tnvasantha123@gmail.com)

which occurs at the solid-fluid interface due to the presence of a slip length, modifies the boundary conditions and can alter the velocity profile near the surface. Viscous dissipation, the conversion of mechanical energy into heat due to fluid friction, generates additional heat within the fluid, impacting the thermal boundary layer and the temperature distribution.

The combined effects of these factors on the MHD flow and heat transfer can be quite intricate. For instance, a favorable pressure gradient can thin the momentum boundary layer, while a slip velocity can thicken it. The interplay of these factors can also influence the heat transfer rate, as the temperature profile within the thermal boundary layer is closely linked to the velocity profile in the momentum boundary layer. Additionally, the presence of a magnetic field introduces Lorentz force, which can further modify the flow and heat transfer characteristics. Boundary layer flows over a moving wedge is a fundamental concept in fluid mechanics that describes the behaviour of a fluid layer near the surface of a wedge-shaped object. The wedge, characterized by its angle, creates a pressure gradient along its surface. This pressure gradient influences the fluid's velocity profile within the boundary layer, which is the thin region of fluid adjacent to the wedge where the velocity varies significantly from the free-stream velocity. The study of boundary layer flow over a wedge has numerous applications in various fields [1–5]. In aerodynamics, understanding this phenomenon is crucial for designing aircraft wings and other aerodynamic surfaces. The angle of the wedge can affect the lift and drag characteristics of the object. In fluid mechanics, boundary layer flow over a wedge is used to study the effects of pressure gradients on boundary layer development and separation. Additionally, in heat transfer, the boundary layer plays a significant role in determining the rate of heat transfer between the wedge and the fluid, which is important in applications such as cooling systems and heat exchangers [6–10]. We study the influence of Prandtl number and Eckert number on the boundary layer flow. Prandtl number Pr is a dimensionless quantity that relates the momentum diffusivity (kinematic viscosity) to the thermal diffusivity of a fluid. It essentially measures the relative importance of momentum transfer and heat transfer within a fluid. A high Prandtl number indicates that momentum diffuses more slowly than heat, which is typical of liquids. Conversely, a low Prandtl number indicates that heat diffuses more slowly than momentum, which is typical of gases. The Prandtl number has significant implications in various fields, including heat transfer, fluid mechanics, convection, and engineering applications. It affects the rate of heat transfer, the development of boundary layers, the type of convection, and the design of various systems, making it a crucial parameter in understanding and analyzing fluid flow and heat transfer phenomena.

The Eckert number is a dimensionless parameter that quantifies the ratio of kinetic energy to enthalpy difference in a fluid flow. It is used to assess the significance of viscous dissipation in heat transfer problems. Viscous dissipation occurs when the kinetic energy of a fluid is converted into internal energy due to friction between fluid particles. This process can lead to a significant increase in the fluid's temperature, especially in high-speed flows or flows with large shear stresses. The influence of Eckert number on viscous dissipation is significant. A high Eckert number indicates that the kinetic

energy of the fluid is relatively large compared to the enthalpy difference, meaning that viscous dissipation is a major factor in the heat transfer process. As a result, the fluid's temperature can increase significantly due to the conversion of kinetic energy into internal energy. Conversely, a low Eckert number indicates that the kinetic energy of the fluid is relatively small compared to the enthalpy difference, meaning that viscous dissipation is less significant in the heat transfer process. In this case, the fluid's temperature increase due to viscous dissipation is relatively small.

The wall exponent parameter N is a dimensionless quantity that appears in the Falkner-Skan equation, which describes the flow of a viscous, incompressible fluid over a wedge-shaped body. It is used to characterize the pressure gradient along the wedge surface. When $N = 0$ corresponds to flow over a flat plate, $N > 0$ represents a favorable pressure gradient, where the pressure decreases in the direction of flow. This can lead to boundary layer growth and potentially separation and $N < 0$ represents an adverse pressure gradient, where the pressure increases in the direction of flow. This can cause the boundary layer to thicken and eventually separate from the surface. The value of N significantly influences the behavior of the boundary layer and the overall flow characteristics. For example, a higher value of N indicates a stronger favorable pressure gradient, which can lead to a thicker boundary layer and increased skin friction. Conversely, a lower value of N indicates a stronger adverse pressure gradient, which can lead to boundary layer separation and increased drag.

Magnetohydrodynamic (MHD) is the study of the interaction between electrically conducting fluids (like plasmas and liquid metals) and electromagnetic fields. When a conducting fluid flows through a magnetic field, an electromagnetic force is induced on the fluid. This force can significantly alter the fluid's behavior, particularly near solid boundaries. MHD boundary layer theory focuses on the region of fluid near a solid surface where the velocity varies significantly from the free-stream velocity due to the interaction with an applied magnetic field. This boundary layer is influenced by both the fluid's viscosity and the electromagnetic forces [11–13].

Slip boundary conditions are used to model the behavior of the fluid at the solid surface. Unlike the traditional no-slip condition, which assumes that the fluid velocity at the surface is zero, slip boundary conditions allow for a non-zero velocity at the surface. This is particularly relevant in MHD flows, especially at high Hartmann numbers or for highly conducting fluids. The combination of MHD boundary layer theory and slip boundary conditions is important in understanding the behaviour of conducting fluids in various applications, such as plasma confinement devices, liquid metal flows, and drag reduction. The slip boundary condition in the Falkner-Skan equation is a modification of the traditional no-slip condition. Instead of assuming that the fluid velocity at the wall is zero relative to the wall, a slip boundary condition allows for a non-zero velocity at the wall. This is particularly relevant in certain flow regimes, such as high-speed flows or flows with a strong magnetic field.

Suction in boundary layer flow refers to the process of removing fluid from the boundary layer. This can be achieved by introducing a suction slot or porous surface at the wall. Suction can help to delay or prevent boundary layer separation, reduce skin friction, and control heat transfer. These

benefits have applications in aerodynamics, turbo machinery, and heat exchangers, where suction can improve performance and efficiency [14–18]. The current work is structured as follows. Section §2 contains the conservation equations for mass, momentum, and energy that lead to the momentum and thermal boundary-layer model. The stream function and similarity transformations are now included in this section. The numerical scheme for solving the governing equations is the focus of Section §3. The different outcomes are simulated and examined using figures in section §4. The specifics of the temperature and velocity gradients on the wall are also shown in Section §4. The results of the current investigation are summarised in the final section.

2. Mathematical Formulation

The two-dimensional magnetohydrodynamics laminar flow of a viscous and incompressible fluid over a stationary wedge with the effects of slip velocity and viscous dissipation is investigated. It is also assumed that the slip velocity which refers to the relative velocity between a moving fluid and a wedge boundary is considered. The Cartesian coordinates are taken with the $x-$ axis is taken along the flow direction and y is normal to the flow. The wedge surface is assumed to have the temperature T_w and mainstream temperature T_∞ with a condition that $T_w \gg T_\infty$. The model is governed by the following governing equations (continuity, momentum and energy transport equations)

$$\nabla \cdot \mathbf{u} = 0 \tag{1}$$

$$\rho(\mathbf{u} \cdot \nabla)\mathbf{u} = -\nabla p + \mu \nabla^2 \mathbf{u} - \mathbf{J} \times \mathbf{B} \tag{2}$$

$$(\mathbf{u} \cdot \nabla)T = \alpha_1 \nabla^2 T + V_d \tag{3}$$

where $\mathbf{u}$ is an intrinsic velocity of the fluid, ρ is the fluid density, p is the pressure, μ is the fluid viscosity, $\mathbf{J} \times \mathbf{B}$ is the Lorentz force with current density $\mathbf{J}$ and magnetic field $\mathbf{B}$, T is the fluid temperature, $\alpha_1 = \frac{\kappa}{\rho c_p}$ is thermal diffusivity with c_p being the specific heat at constant pressure and κ is thermal conductivity, and V_d is the viscous dissipation in the model. Since both the momentum and thermal boundary layers occur close to the wedge surface, it is considered that the Reynolds number of the fluid is asymptotically large. The viscous effects are more pronounced in the area close to the wedge surface and gradually diminish to zero farther away from it in the momentum boundary layer. With respect to the model described above, when using the standard boundary-layer approximations the system (1)-(3) has the following form [19]

$$\frac{\partial u}{\partial x} + \frac{\partial v}{\partial y} = 0 \tag{4}$$

$$u\frac{\partial u}{\partial x} + v\frac{\partial u}{\partial y} = -\frac{1}{\rho}\frac{\partial p}{\partial x} + \nu\frac{\partial^2 u}{\partial y^2} - \frac{\sigma B_0^2}{\rho}u \tag{5}$$

$$0 = \frac{\partial p}{\partial y} \tag{6}$$

$$u\frac{\partial T}{\partial x}+v\frac{\partial T}{\partial y}=\alpha\frac{\partial^2 T}{\partial y^2}+V_d. \tag{7}$$

Here, the velocity components u, v are taken along x and y directions, $\nu(=\frac{\mu}{\rho})$ is the kinematics viscosity of the fluid, σ is the electrical conductivity, B_0 is the applied magnetic field. The viscous dissipation V_d is defined as $V_d=\frac{\nu}{c_p}(\frac{\partial u}{\partial y})^2$. Note that the velocity in the boundary layer is expected to approach the mainstream flow at the edge of the boundary layer that is $u(x,y)=U(x)$. Accordingly, the pressure variation normal to the wedge is treated as constant and whence obtain

$$U\frac{dU}{dx}=-\frac{1}{\rho}\frac{\partial p}{\partial x}-\frac{\sigma B_0^2}{\rho}U \tag{8}$$

where $U(x)$ is a mainstream velocity away from the boundary layer. It is approximated that the mainstream flow has a variation in the power of distance from the leading edge i.e. $U(x)=U_\infty x^m$ where U_∞ is constant and positive always and m is related to the imposed pressure gradient. Thus, equation (5) may be rewritten in view of (8) as

$$u\frac{\partial u}{\partial x}+v\frac{\partial u}{\partial y}=U_\infty^2 x^{2m-1}+\nu\frac{\partial^2 u}{\partial y^2}+\frac{\sigma B_0^2}{\rho}(U-u). \tag{9}$$

To render the physical solution for the above mode, we define the relevant boundary conditions in the following manner

$$u=\mu S\frac{\partial u}{\partial y},\qquad v=V_w,\ \ T=T_w,\qquad \text{at } y=0, \tag{10}$$

$$u=U,\qquad T=T_\infty,\quad \text{as } y\to\infty \tag{11}$$

where the parameter S is the slip velocity which is the relative velocity between the wedge and fluid, V_w is suction or injection parameter in which for suction it is $V_w>0$ and for injection it is $V_w<0$ while $V_w=0$ gives the impermeable wedge surface. The boundary conditions characterize the flow velocity u and temperature T to decay in an asymptotic manner onto the mainstream velocity U and temperature T_∞. We assume that the temperature varies from wedge temperature to the mainstream in the manner $T_w=T_\infty+Ax^N$ where A is positive constant and N is the wall exponent parameter.
In order to obtain the physically meaningful solutions, we take the velocity components u and v in the following manner

$$u=\frac{\partial\psi}{\partial y}\quad\text{and}\quad v=-\frac{\partial\psi}{\partial x} \tag{12}$$

which are found to satisfy the continuity equation, where $\psi(x,y)$ is the stream function. We define the new similarity variables in the following manner

$$\psi=\left(\frac{2\nu xU}{m+1}\right)^{\frac{1}{2}}\phi(\eta),\ \ \frac{T-T_\infty}{T_w-T_\infty}=\theta(\eta),\ \ \eta=\left(\frac{(m+1)U}{2\nu x}\right)^{\frac{1}{2}}y \tag{13}$$

where $\phi(\eta)$, $\theta(\eta)$ and η are a new set of similarity transformations. Using the similarity transformations (13) in the momentum and energy equation (9) and (7), we get

$$\phi'''(\eta) + \phi(\eta)\phi''(\eta) + \beta(1 - \phi'^2(\eta)) + (2-\beta)M^2(\phi'(\eta) - 1) = 0 \tag{14a}$$

$$\theta''(\eta) + Pr\phi(\eta)\theta'(\eta) - (2-\beta)PrN\phi'(\eta)\theta(\eta) + PrEc\phi''^2(\eta) = 0 \tag{14b}$$

and transformed boundary conditions (10)-(11) take the form

$$\phi(0) = s, \;\; \phi'(0) = K\phi''(0), \;\; \theta(0) = 1 \tag{15a}$$

$$\phi'(\infty) = 1, \;\; \theta(\infty) = 0 \tag{15b}$$

where $\phi = \phi(\eta)$ and $\theta = \theta(\eta)$ are the non-dimensional stream functions and primes denote differentiation with respect to η. When $M = 0$ and $s = 0 = K$, the most celebrated Falkner-Skan boundary layer flow over a wedge is recovered [3,20]. The various parameters along with their importance in the applications in the above system are given below:

1. The parameter $\beta = 2m/(m+1)$ is the pressure gradient in that $\beta < 0 (> 0)$ is a decelerated (accelerated) pressure gradient and $\beta = 0$ gives the flow over a flat plate.

2. The variable $M = \sqrt{\frac{\sigma}{\rho U_\infty}} B_0$ is the magnetic number. It is the ratio of electromagnetic force to the viscous force where $M = 0$ represents the flow in the absence of the magnetic field and $M > 0$ for the influence of the magnetic field.

3. The Prandtl number $Pr = \frac{\nu}{\alpha}$ infers for $Pr < 1$ and $Pr > 1$ as the thickness of the thermal boundary layer is larger and smaller compared to the thickness of the boundary layer whereas $Pr = 1$ is the case for identical boundary layers.

4. The parameter s is the suction/injection parameter which determines the transpiration rate of the surface where $s < 0$ (> 0) as injection (suction) and $s = 0$ has no transpiration or the surface is impermeable.

5. The slip velocity $K = S\mu\sqrt{\frac{U_\infty}{\nu}}$ describes the relative importance between the magnitude of the slip velocity at the fluid-surface interface and mainstream velocity of the fluid away from the surface and $K > 0$.

6. The Eckert number $Ec = \frac{U^2}{c_p(T_w - T_\infty)}$ is defined as the ratio of the kinetic energy of a fluid to its thermal energy. And

7. The parameter N is the wall exponent parameter which signifies how the heat transfer coefficient varies with distance from the wedge wall.

The system (14) - (15) is highly non-linear coupled ordinary differential equations defined in the boundary layer domain $[0, \infty)$ and hence solved them numerically using the shooting method since any analytical solution is almost impossible.

3. Numerical Procedure

We employ the shooting approach to numerically simulate the physically authentic solutions of the considered model. The shooting method [21], a hybrid approach that combines the Secant and Runge-Kutta methods, entails the following steps: We initially add some more unknown functions to the boundary value problems in order to transform them into the initial value problem. That is

$$\phi'(\eta) = \phi_1(\eta), \qquad \phi_1'(\eta) = \phi_2(\eta), \qquad \theta'(\eta) = \theta_1(\eta) \tag{16}$$

$$\phi_2'(\eta) = -\phi(\eta)\phi_2(\eta) - \beta(1 - \phi_1^2(\eta)) - (2-\beta)M^2(\phi_1(\eta) - 1) \tag{17}$$

$$\theta_1'(\eta) = -\Pr\phi(\eta)\theta_1(\eta) + (2-\beta)PrN\phi_1(\eta)\theta - PrEc\phi_2^2(\eta) \tag{18}$$

along with the boundary conditions

$$\phi(0) = s, \quad \phi_1(0) = K\phi_1'(0), \quad \theta(0) = 0, \quad \phi_1(\infty) = 1, \quad \theta(\infty) = 0 \tag{19}$$

The above-converted system is then integrated from the wedge surface to the boundary layer edge using the Runge-Kutta method, assuming initial guesses for $\phi_2(0)$ and $\theta_1(0)$. The temperature gradient $\theta_1(0)$ and wall-shear stress $\phi_2(0)$ receive their significant initial guesses from the secant method technique. The usual secant approach is used to accelerate the necessary solutions for $\phi_2(0)$ and $\theta_1(0)$ on the wedge surface. When there is no discernible difference between two successive solutions up to the pre-specified error tolerance, which in the current experiments is 10^{-5}, the shooting procedure is stopped. The physically authentic profiles are obtained at this point of convergence and are covered in detail in the sections that follow.

4. Results and Discussion

We have examined the combined impacts of the magnetic number, pressure gradient, slip velocity, and viscous dissipation numerically on the two-dimensional boundary layer flow over a wedge. The magnetohydrodynamic boundary-layer flow velocity and temperature distribution, as well as the impacts of various values of the momentum slip parameter K, suction-injection s, magnetic number M, Prandtl number Pr, Eckert number Ec, and other numbers, are derived. With the help of the similarity variables, a system of ordinary differential equations with suitable boundary conditions has been created from the thermal and momentum boundary layer equations (7) and (9). The numerical technique is validated for multiple parameters by repeatedly checking and verifying its correctness

and grid independence test. Dimensionless velocity $\phi(\eta)$, temperature $\theta(\eta)$, skin-friction $\phi''(0)$, and temperature gradient $\theta'(0)$ all have physical answers for emergent parameters as a result of the numerical solutions.

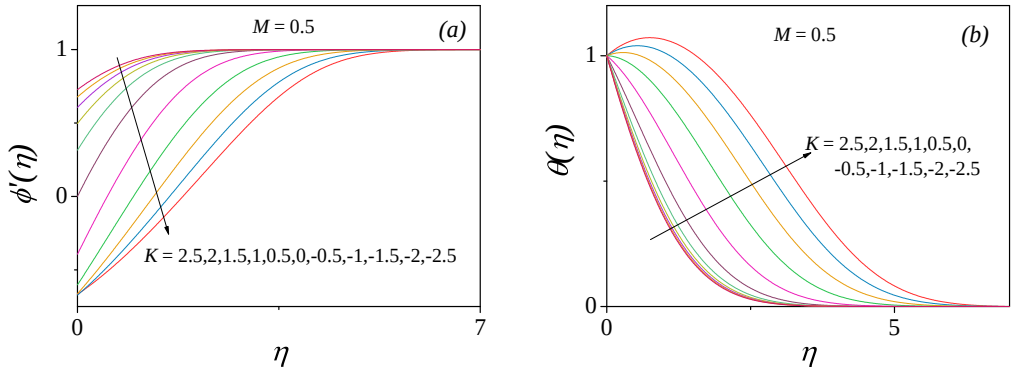

Figure 1: The variation of (a) the velocity and (b) the temperature profiles with η for different values of K with $\beta = 0.5$, $M = 0.5$, $s = 0$, $Ec = 0.5$, $Pr = 0.7$ and $N = 0.4$.

The impact of slip velocity boundary conditions on the flow of the boundary layer and the corresponding rate of heat transfer is examined. The slip velocity K for the velocity and thermal profiles are displayed at $M = 0.5$ and $s = 0$ in figures 1a-1b, with the slip velocity falling between -2.5 with 2.5. Returning to $K = 0$, the case of well-known no-slip condition is recovered. The velocity curves are shown to decay to their mainstream conditions, despite the fact that they start at different places due to the boundary conditions stated in (15b). The surface-proximate boundary layer thickness is clearly changed by increasing K. Due to the fluid near the moving wedge flowing more quickly as a result of the viscous effects being more pronounced, this appears to thin the boundary layer. Furthermore, it is seen that the slip velocity is the reason for the noticeable difference in velocity between the boundary layer edge and the surface, which increases with decreasing K. The thermal boundary layer is observed to be altered since the fluid's temperature is also dependent on its velocity, which is controlled by the slip velocity.

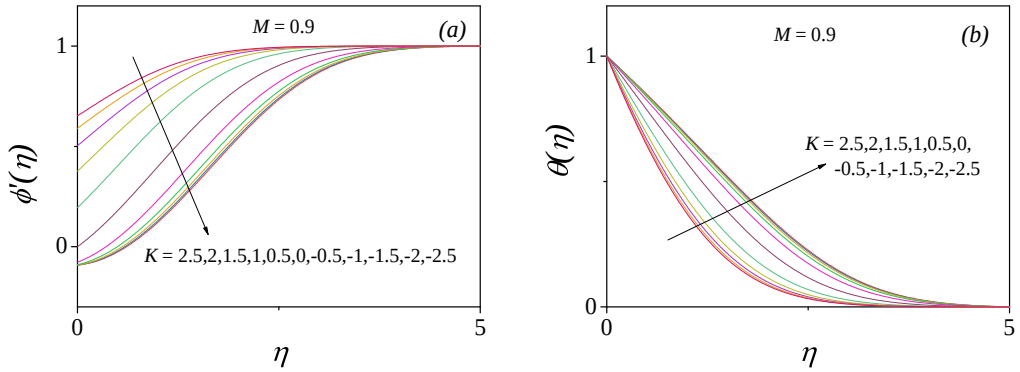

Figure 2: The variation of (a) the velocity and (b) the temperature profiles with η for different values of K with $\beta = 0.5$, $M = 0.9$, $s = 0$, $Ec = 0.5$, $Pr = 0.7$ and $N = 0.4$.

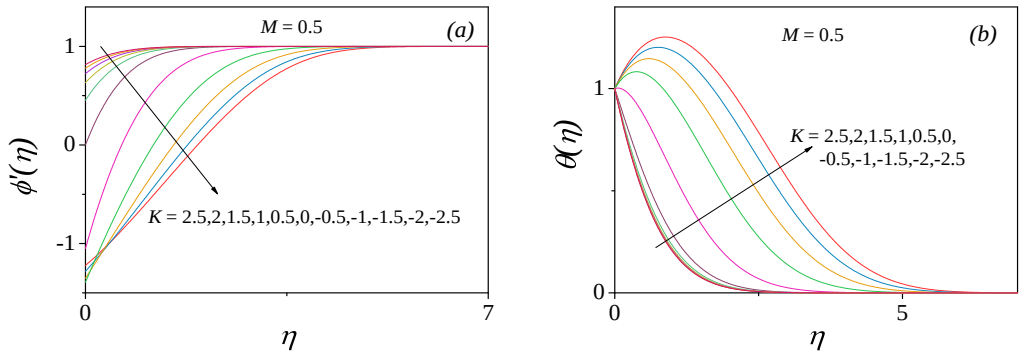

Figure 3: The variation of (a) the velocity and (b) the temperature profiles with η for different values of K with $\beta = 0.5$, $M = 0.5$, $s = 1$, $Ec = 0.5$, $Pr = 0.7$ and $N = 0.4$.

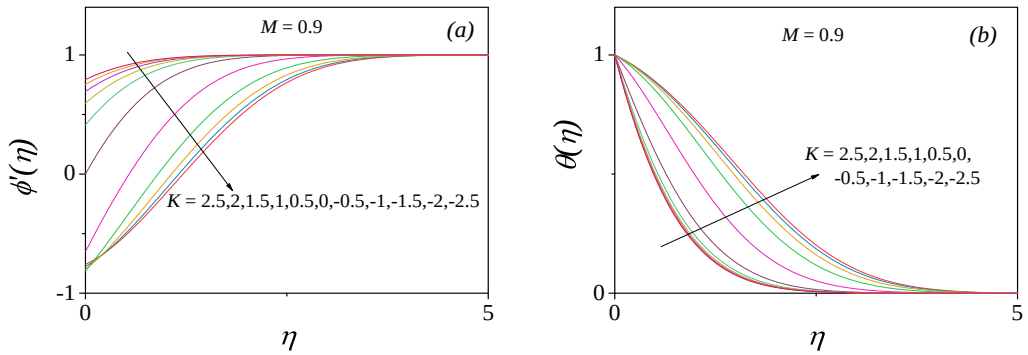

Figure 4: The variation of (a) the velocity and (b) the temperature profiles with η for different values of K with $\beta = 0.5$, $M = 0.9$, $s = 1$, $Ec = 0.5$, $Pr = 0.7$ and $N = 0.4$.

Figure 1b illustrates that for lower K, there is an altered velocity contribution and an improved rate of heat transfer because of the thicker thermal boundary layer. Similar shaped velocity and temperature profiles can be observed for $M = 0.9$ and $s = 0$ in figures 2a - 2b, where the boundary layer is rather thick, but the physical mechanisms for this selected M stay the same. Also, we see similar velocity and temperature shapes for suction parameter $s = 1$ in figures 3(a-b) - 4(a-b) for $M = 0.5$ and $M = 0.9$ respectively. However, the boundary layer thickness decreases with increasing magnetic field M and the velocity of the fluid increases in the boundary layer regime. It is noticed that the interesting phenomenon occurring in thermal profiles of figure 3, corresponds to an overshoot profile for decreasing slip parameter K. These genuine structures of $\theta(\eta)$ enhance the fluid flow at low magnetic effects while this scenario deprives the flow at magnetic number $M = 0.9$ as shown in figure 4.

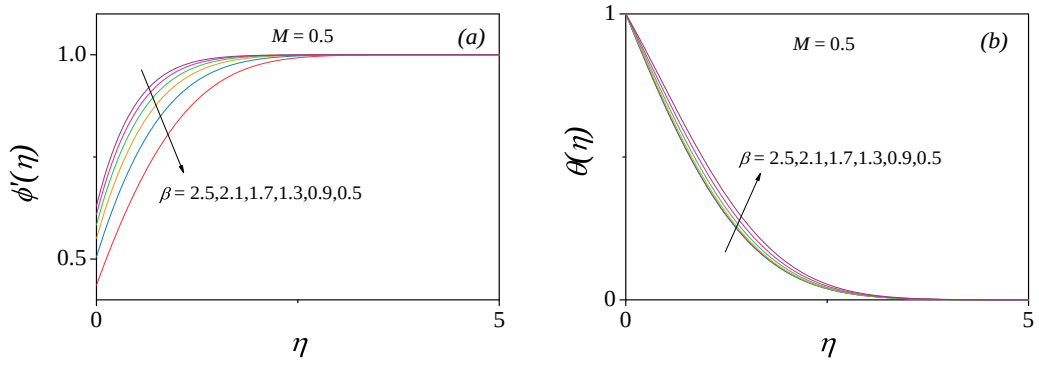

Figure 5: The variation of (a) the velocity and (b) the temperature profiles with η for different values of β with $K = 0.8$, $M = 0.5$, $s = 0$, $Ec = 0.5$, $Pr = 0.7$ and $N = 0.4$.

For increasing values of β at $M = 0.5$, as shown in figure 5, under the influence of a magnetic field the favourable pressure gradient for which pressure in the direction of flow decreases and promotes benign flow making the boundary layer attached to the wedge. With a favourable pressure gradient parameter, the boundary layer thickness is small, as expected, as the flow for $\beta > 0$ gradually accelerates down the wedge surface, minimizing viscous effects. Interestingly, when $\beta > 0$, all velocity profiles asymptotically meet the boundary criteria. The accelerated pressure gradient, on the other hand, has a significant influence on the thermal boundary layer, which is projected to vary between the wedge temperature and the mainstream temperature, with only a minor change near the surface. For a favourable pressure gradient $\beta > 0$, the thermal boundary layer is thin because fluid flow accelerates smoothly down the wedge surface, resulting in an increased heat transfer rate. However, when the magnetic field is increased sufficiently up to $M = 0.9$, similar solution structures are observed for the velocity and thermal profiles with the advancement of the fluid flow in the magnetohydrodynamic thermal boundary layer as seen in figure 6.

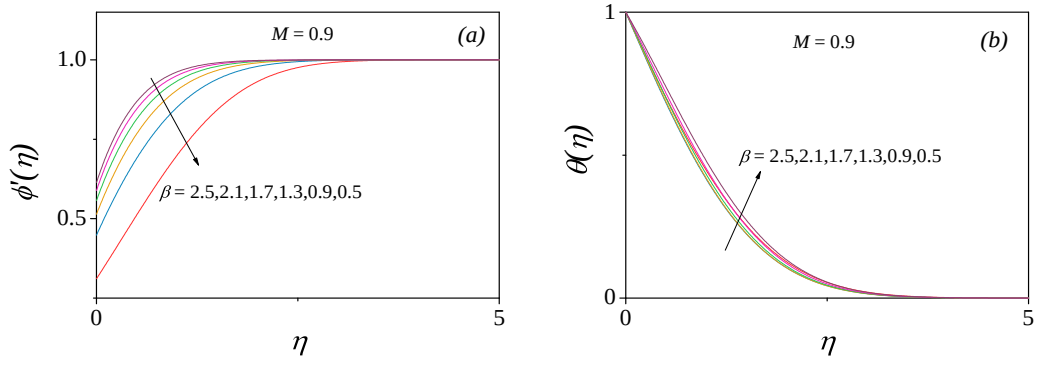

Figure 6: The variation of (a) the velocity and (b) the temperature profiles with η for different values of β with $K = 0.8$, $s = 0$, $Ec = 0.5$, $Pr = 0.7$ and $N = 0.4$.

Further, the shapes of the velocity profiles for $s = 1$ for different M remain to persist in the same nature as of $s = 0$. The profiles are plotted in the figures 7(a-b) and 8(a-b) respectively for their corresponding velocity shapes and thermal shapes as subfigures for magnetic numbers $M = 0.5$ and

$M = 0.9$ respectively.

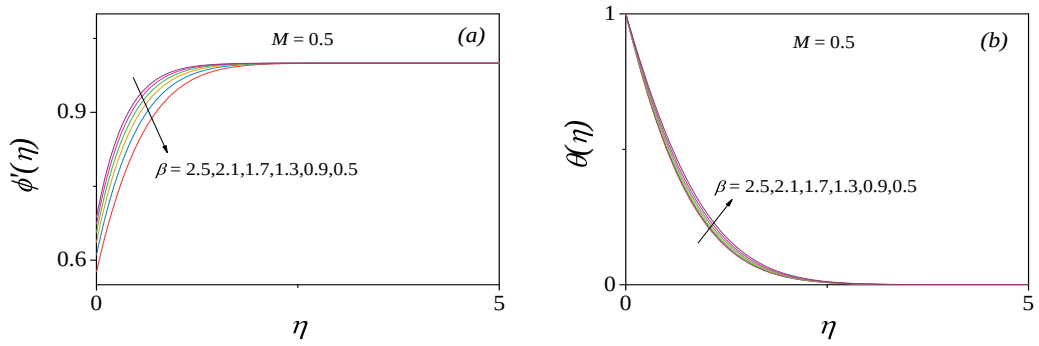

Figure 7: The variation of (a) the velocity and (b) the temperature profiles with η for different values of β with $K = 0.8$, $M = 0.5$, $s = 1$, $Ec = 0.5$, $Pr = 0.7$ and $N = 0.4$.

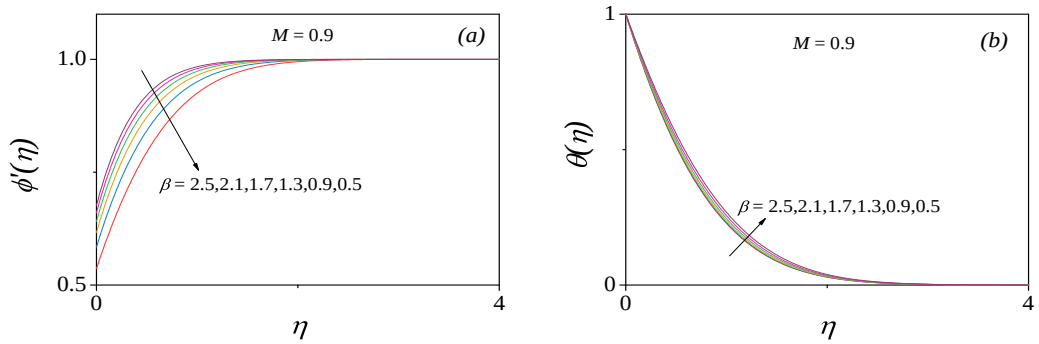

Figure 8: The variation of (a) the velocity and (b) the temperature profiles with η for different values of β with $K = 0.8$, $M = 0.9$, $s = 1$, $Ec = 0.5$, $Pr = 0.7$ and $N = 0.4$.

Regardless, the boundary layer thickness advances as the magnetic field is varied appropriately. Although the magnetic number M contribution does not appear in the equation (14b) directly, there is a small portion of variations are seen in the thermal profiles of the figures 7b and 8b due to the ordinary differential equation (14a) is affecting equation (14b). Thus, slight variations are still observed for increasing β and M. This is further confirmed in the velocity and thermal profiles in figure 9.

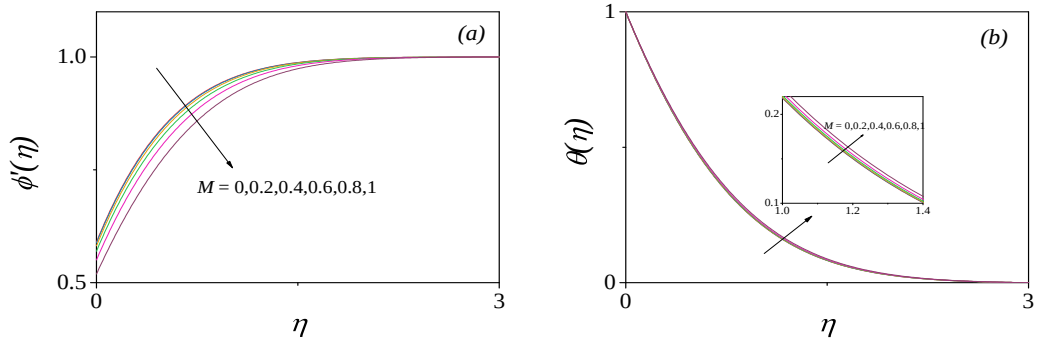

Figure 9: The variation of (a) the velocity and (b) the temperature profiles with η for different values of M with $K = 0.8$, $\beta = 0.5$, $s = 1$, $Ec = 0.5$, $Pr = 0.7$ and $N = 0.4$.

We shall now discuss the variations due to the magnetic number M. The shapes obtained from the velocity and thermal profiles vary in the momentum and thermal boundary layer and the velocity of the fluid increases thereby making the boundary layer thinner. With an increase in the magnetic effect, the particles in the fluid get magnetized and the energy in the system is enhanced, as a result, the velocity of the particles increases as seen in figure 9a. In figure 9b, there is a very small amount of heat transfer taking place due to the influence of the magnetic field in the system as the magnetic field is only affecting the velocity of the fluid particles.

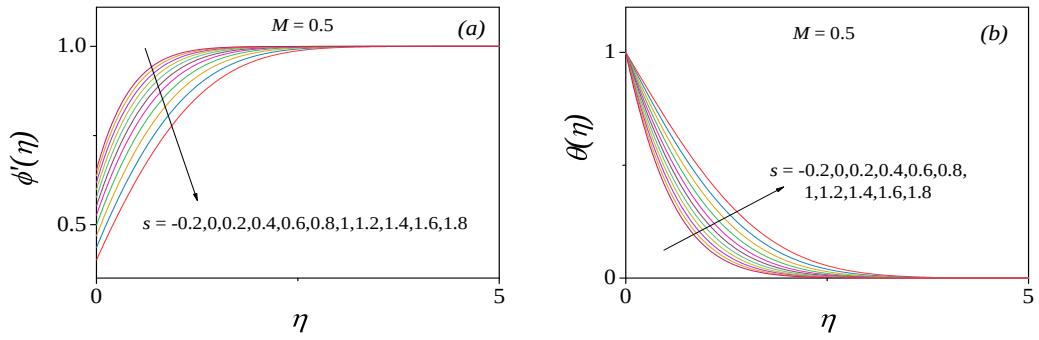

Figure 10: The variation of (a) the velocity and (b) the temperature profiles with η for different values of s with $K = 0.8$, $\beta = 0.5$, $M = 0.5$, $Ec = 0.5$, $Pr = 0.7$ and $N = 0.4$.

In contrast to these results, we have encountered that the velocity and thermal profiles show an evident difference in the shapes of the profiles for suction $s > 0$ and injection $s < 0$ with magnetic field in the figures 10-11.

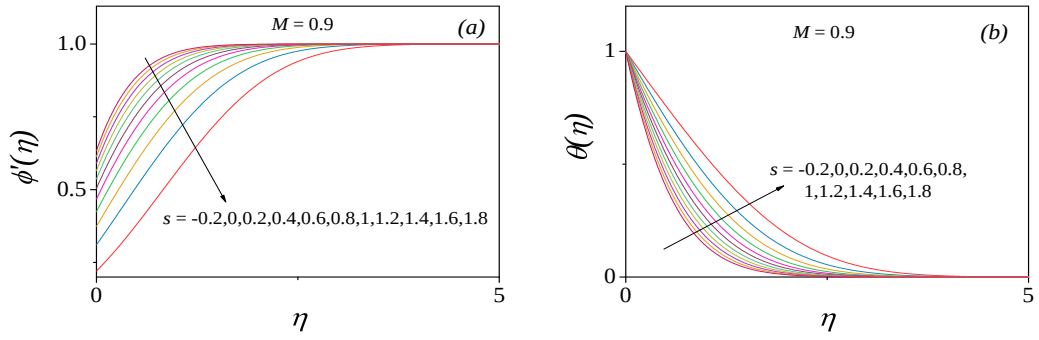

Figure 11: The variation of (a) the velocity and (b) the temperature profiles with η for different values of s with $K = 0.8$, $\beta = 0.5$, $M = 0.9$, $Ec = 0.5$, $Pr = 0.7$ and $N = 0.4$.

It is expected that the suction thickens the boundary layer and injection thins it i.e. due to increasing s, the velocity of the fluid increases. By sucking the particles of the fluid through the porous wedge the growth of the boundary layer gets reduced. The momentum boundary layer reduces due to the effect of suction $s > 0$ that helps in sucking the fluid near the wedge, for which the fluid velocity increases while the opposite trend is observed for the injection $s < 0$. It shows how, in the presence of slip at the boundary layer, the suction parameter s affects temperature and velocity profiles, respectively. The results show that while fluid velocity increases with blowing, it reduces noticeably with increasing

suction parameters (figures 10a and 11a). It is found that the boundary layer thickness and velocity field diminish when the wall suction $(s > 0)$ is taken into account. The scenario of a non-porous wedge is represented by $s = 0$. When $s < 0$ is blown, the opposite behaviour is observed. The thickness of the thermal boundary layer decreases with an increase in s that pronounces the heat transfer rate.

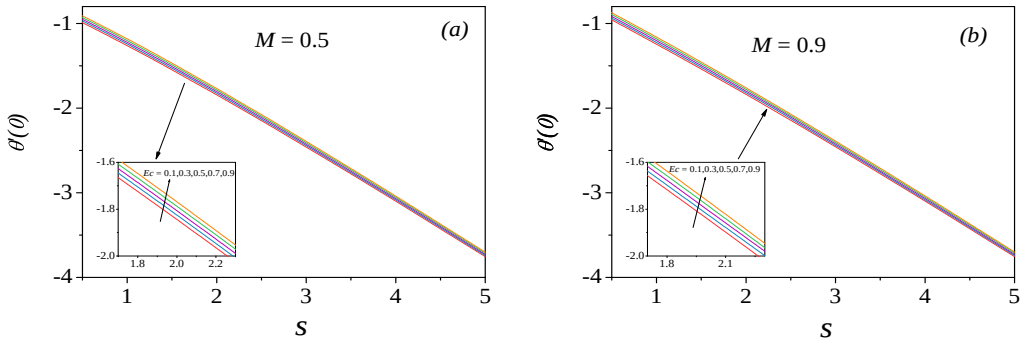

Figure 12: The temperature gradient versus suction-injection for different values of Ec with fixed $K = 0.8$, $Pr = 0.7$, $N = 0.4$, $\beta = 0.5$, (a) $M = 0.5$ and (b) $M = 0.9$.

The wall shear stress or skin-friction $\phi''(0)$ and the temperature gradient $\theta'(0)$ can be used to understand the broader structure of the nature of Eckert number Ec and slip-velocity K. We discuss various results in terms of these two parameters, which are important for engineering interest and are discussed for pressure gradient and viscous dissipation. The values of $\phi''(0)$ and $\theta'(0)$ are obtained by numerical method and exhibited with the suction-injection parameter s. In figures 12a-12b, we demonstrate the gradient of temperature for various Eckert number Ec in the influence of magnetic field.

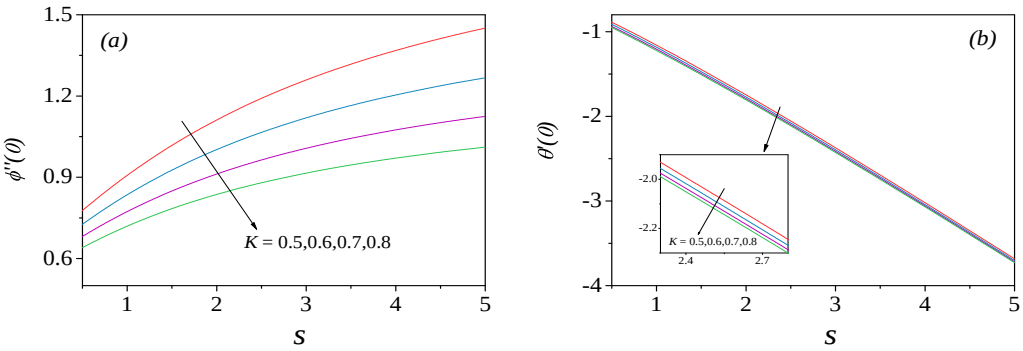

Figure 13: The wall shear stress and temperature gradient versus suction-injection for different values of K with fixed $M = 0.5$, $Ec = 0.5$, $Pr = 0.7$, $N = 0.4$, $\beta = 0.5$.

Note that for each of these values, there are both velocity and temperature variations but there are marginal variations in velocity profiles for different Ec, thus it is not shown in the figures. For each Ec considered with $M = 0.5$ and $M = 0.9$, the temperature gradients on the surface are seen to decrease gradually for increasing suction-injection parameter s. These variations for different Ec have very small differences, therefore, it is enlarged and shown as a subfigure in each panel of the figures. It is seen that when the Eckert number is increased from 0.1 to 0.7, there is a decrease in the temperature gradient,

which simulates the heat transfer into the boundary layer (figure 12a). This situation is upheld for $M = 0.9$ as seen in the figure 12b.

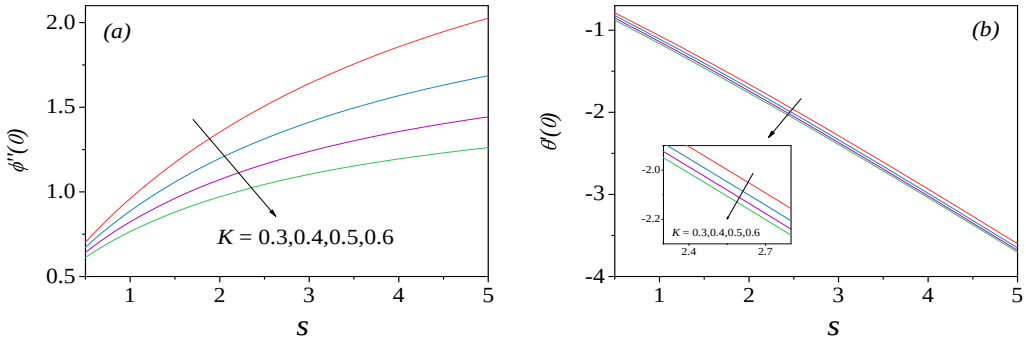

Figure 14: The wall shear stress and temperature gradient versus suction-injection for different values of K with fixed $M = 0.9$, $Ec = 0.5$, $Pr = 0.7$, $N = 0.4$, $\beta = 0.5$.

Figures 13 and 14 illustrate the gradients of velocity and temperature for slip velocity K in the effect of the magnetic field at $M = 0.5$ (figure 13) and $M = 0.9$ (figure 14). There is an evident difference for the wall shear-stress $\phi''(0)$ when slip velocity K is increased for varying suction-injection parameter s. There is an exponential increase of $\phi''(0)$ whereas a slight difference in temperature gradient $\theta'(0)$, thus, a portion of curves is enlarged as a subfigure in the figures. However, we can see the temperature gradient values are decreasing for increasing Ec for both magnetic number M.

References

[1] B. C. Sakiadis, *Boundary-layer behavior on continuous solid surfaces: I. Boundary-layer equations for two-dimensional and axisymmetric flow*, AIChE Journal, 7(1)(1961), 26-28.

[2] Lawrence J Crane, *Flow past a stretching plate*, Zeitschrift ful angewandte Mathematik und Physik ZAMP, 21(1970), 645-647.

[3] N. Riley and P. D. Wiedman, *Multiple solutions of the Falkner-Skan equation for a flow past a stretching boundary*, SIAM Journal on Applied Mathematics, 49(5)(1989), 1350-1358.

[4] N. Afzal, A. Badaruddin and A. A. Elgarvi, *Momentum and heat transport on a continuous flat surface moving in a parallel stream*, International Journal of Heat and Mass Transfer, 36(13)(1993), 3399-3403.

[5] P. L. Sachdev, R. B. Kudenatti and N. M. Bujurke, *Exact analytic solution of a boundary value problem for the Falkner-Skan equation*, Studies in Applied Mathematics, 120(1)(2008), 1-16.

[6] A. Ishak, R. Nazar and I. Pop, *The effects of transpiration on the flow and heat transfer over a moving permeable surface in a parallel stream*, Chemical Engineering Journal, 148(1)(2009), 63-67.

[7] Andreas Acrivos, *On the combined effect of forced and free convection heat transfer in laminar boundary layer flows*, Chemical Engineering Science, 21(4)(1966), 343-352.

[8] ERG Eckert, *Engineering relations for heat transfer and friction in high-velocity laminar and turbulent boundary-layer flow over surfaces with constant pressure and temperature*, Transactions of the American Society of Mechanical Engineers, 78(6)(1956), 1273-1283.

[9] Krishnendu Bhattacharyya, *Boundary layer flow and heat transfer over an exponentially shrinking sheet*, Chinese Physics Letters, 28(7)(2011), 074701.

[10] Mohd Zuki Salleh, Roslinda Nazar and I Pop. *Boundary layer flow and heat transfer over a stretching sheet with newtonian heating*, Journal of the Taiwan Institute of Chemical Engineers, 41(6)(2010), 651-655.

[11] Govind R Rajput, Bipin P Jadhav, and S. N. Salunkhe, *Magnetohydrodynamics boundary layer flow and heat transfer in porous medium past an exponentially stretching sheet under the influence of radiation*, Heat Transfer, 49(5)(2020), 2906-2920.

[12] A Ogulu and J Prakash, *Heat transfer to unsteady magneto-hydrodynamic flow past an infinite moving vertical plate with variable suction*, Physica Scripta, 74(2)(2006), 232.

[13] Fadzilah Md Ali, Roslinda Nazar, Norihan Md Arifin and Ioan Pop, *Mhd boundary layer flow and heat transfer over a stretching sheet with induced magnetic field*, Heat and Mass transfer, 47(2011), 155-162.

[14] Robert Middleton Terrill, *Laminar boundary-layer flow near separation with and without suction*, Philosophical Transactions of the Royal Society of London. Series A, Mathematical and Physical Sciences, 253(1022)(1960), 55-100.

[15] R. A. Antonia, Y. Zhu, and M. Sokolov, *Effect of concentrated wall suction on a turbulent boundary layer*, Physics of Fluids, 7(10)(1995), 2465-2474.

[16] N. G. Kafoussias and N. D. Nanousis. *Magnetohydrodynamic laminar boundary-layer flow over a wedge with suction or injection*, Canadian Journal of Physics, 75(10)(1997), 733-745.

[17] R. B. Kudenatti, S. R. Kirsur, L. N. Achala and N. M. Bujurke, *MHD boundary layer flow over a non-linear stretching boundary with suction and injection*, International Journal of Non-Linear Mechanics, 50(2013), 58-67.

[18] Muhammad Ijaz Khan, Muhammad Tamoor, Tasawar Hayat and Ahmed Alsaedi. *Mhd boundary layer thermal slip flow by nonlinearly stretching cylinder with suction/blowing and radiation*, Results in Physics, 7(2017), 1207-1211.

[19] S. W. Yuan, *Foundations of fluid mechanics*, Prentice-Hall of India, New-Delhi, India, (1988).

[20] H. Schlichting and Gersten, *Fundamentals of boundary-layer theory*, Boundary-layer theory, (2000), 29-49.

[21] J. D. Faires and R. L. Burden, *Numerical methods*, Thomson/Brooks/Cole, (2015).